


Foundation for adaptive charging solutions: Optimised use of electric vehicle charging capacity

Toni Simolin¹  | Kalle Rauma² | Antti Rautiainen¹ | Pertti Järventausta¹ | Christian Rehtanz²

¹Unit of Electrical Engineering, Tampere University, Tampere, Finland

²Institute of Energy Systems, Energy Efficiency and Energy Economics, TU Dortmund University, Dortmund, Germany

Correspondence

Toni Simolin, Unit of Electrical Engineering, Tampere University, Korkeakoulunkatu 7, 33720 Tampere, Finland.
Email: toni.simolin@tuni.fi

Funding information

Bundesministerium für Verkehr und Digitale Infrastruktur

Abstract

As electric vehicles (EVs) are emerging, smart and adaptive charging algorithms have become necessary to ensure safe and efficient operation of the grid. In the scientific literature, most of the proposed charging control algorithms focus solely on EV usage-related behaviour, while the charging characteristics of EVs are overlooked. Herein, realistic charging characteristics are illustrated and discussed. More notably, to overcome the issues caused by the non-idealities in charging characteristics, a new adaptive charging characteristics expectation algorithm is proposed. The objective of this algorithm is to enable accurate estimation of the non-ideal charging characteristics. This can be used to reallocate any unused charging capacity and to ensure that the intended total capacity is used effectively. The effectiveness of the proposed algorithm is demonstrated using hardware-in-the-loop simulations with commercial EVs and real charging data. The results show that the proposed algorithm achieves an 88%–97% capacity usage rate, while the current benchmark solution achieves only 45%.

1 | INTRODUCTION

As electric vehicles (EVs) are emerging at a fast pace, smart charging solutions are becoming increasingly important. When it comes to real-life EV charging solutions, there are often numerous unknown variables to be considered. These unknown variables include the EV user-dependent charging behaviour (available charging time and energy requirement) and the EV technology-dependent charging characteristics, which define the current consumption at each moment of time. Herein, the term ‘charging characteristics’ is used to describe the complex correlation of the realised charging currents to the factors, such as the current limit set by the electric vehicle supply equipment (EVSE), the temperature and state-of-charge (SOC) of the EV battery, and the limitations of the on-board charger (OBC). For the development of efficient smart charging solutions, consideration of realistic charging behaviours and charging characteristics is imperative.

1.1 | Related research and motivation

In the scientific literature, the EV charging behaviour has been analysed from the EV use perspective (hourly/daily level) by using, for example, traffic survey data [1–8], energy metre-level data [9], and actual measurements of charging sessions [6, 10–13]. However, in addition to the differences in EVs' usage, the EVs also have different charging characteristics. It is often assumed that the EV charging current can be fully controlled, but in reality, the EVSE can only set the maximum charging current, and the EV can choose any charging current below the limit. There are several reasons for an EV to charge with a lower current than the limit set by the EVSE such as the vehicle's maximum charging rate being lower than the limit or the OBC may choose a lower charging rate to protect the battery from overheating [14]. The impacts of all these reasons are referred to as non-ideal charging characteristics as the charging current deviates from the current limit set by the EVSE.

This is an open access article under the terms of the Creative Commons Attribution License, which permits use, distribution and reproduction in any medium, provided the original work is properly cited.

© 2021 The Authors. *IET Smart Grid* published by John Wiley & Sons Ltd on behalf of The Institution of Engineering and Technology.

From previous studies [1–14], only [4, 14] mention non-ideal charging characteristics, whereas the rest focus solely on EV usage-related behaviour. In [14], the realised charging currents are measured to determine the energy levels of the EVs more accurately. However, there is no mention of real-locating the unused charging capacity when an EV is drawing less current than the set limit. In [4], experimental measurements of a Citroen C-Zero are used to form a simplified model for the final charging curve. However, no other non-ideal charging characteristics are considered, and the same model is assumed for each EV in the simulations.

The issue regarding the non-idealities has recently been brought up in [15–17] and a solution is presented in [16, 17]. In [15], the final charging curves of 304 charging sessions are analysed. According to the analysis the different charging curves can be classified into six types with reasonable accuracy. In [16], a data-driven approach for integrating a machine learning model to predict the charging profiles is proposed. According to that study, the realised utilisation rate of the charging capacity was 65.8% of the planned utilisation when the EVs are assumed to draw the maximum power, whereas the proposed prediction algorithm achieves a 94.4% utilisation rate. The increased capacity usage rate leads to a higher charging energy dispatch and higher final SOC for the EVs in a limited infrastructure without the need for costly upgrades of the charging infrastructure [16]. Thus, these results signify the importance of the consideration of the non-ideal characteristics. However, even though the results of the proposed solution are very promising, there is a notable drawback. The approach requires a large data set of the charging processes of the EVs and the trained model only reflects the charging characteristics of the models included in the data set. Therefore, its usability might be restricted if the necessary data are not available. In [17], a capacity reallocation algorithm is proposed for a case considering two EVs and a peak power-based tariff. The algorithm is tested using hardware-in-the-loop (HIL) simulations with commercial EVs. The results show that the algorithm effectively reallocates unused charging capacity. However, the algorithm is limited to only two single-phase EVs and the reallocation method is not scalable to a larger charging site.

In public charging stations, it is not reasonable to assume that the charging characteristics of individual EVs can be accurately predicted in advance. In addition, the charge point operators do not have access to internal battery variables [16]. A control system can be made without feedback of the charging current measurements, but this does not enable the control algorithm to observe the realised charging load. The potential deviation between the planned loading and the realised loading is especially significant when considering three-phase charging points [16], because a notable share of all EVs (include both full EVs and plug-in hybrid EVs) support only single-phase charging. By measuring the charging currents, the control algorithm can learn or adapt to the charging characteristics of each EV during the charging sessions, which can then be used for optimisation purposes. Control algorithms with an ability to adapt and learn have been studied

before in, for example, [18–27]. However, the adaptation and learning in these studies focus on the usage-related behaviour, while the limitations caused by the non-ideal charging characteristics are overlooked.

When it comes to practical solutions that are compatible with the charging standards and commercial EVs, the present state-of-the-art solution is to assume that each active EV draws the current indicated by the EVSE, as in [28, 29]. An EV being active refers to a situation where it is plugged in and ready to receive energy. Both these studies acknowledge the fact that the realised charging currents of the EVs may be well below the limit set by the EVSE. In [28], the realised charging currents are measured and used to calculate the realised energy consumption of the EVs, but neither of the studies offers any solutions to reallocate the unused charging capacity.

Based on the literature review, it seems that the non-ideal charging characteristics and their impacts are attracting more attention. However, according to the best knowledge of the authors, practical and scalable solutions to overcome the potential deviation between the planned and realised loading have not been proposed. This kind of solution can increase the charging capacity utilisation rate, which may reduce the necessary investment cost of the local electric grid or improve the quality of the charging service (QoCS), that is, increase the charged energy [16]. A greater charged energy also improves the utilisation rate of the charging points and can lead to higher revenues for the charging operator if a volumetric charging energy pricing is used. In addition, the deviation between the planned and realised loading may have negative impacts on smart charging objectives, such as frequency regulation.

1.2 | Contributions

The aim herein is to thoroughly illustrate the non-ideal charging characteristics and discuss their impacts. More importantly, an adaptive charging characteristics expectation (CCE) algorithm is proposed to minimise the wasted capacity caused by the non-idealities. This is a crucial step towards capacity-efficient charging sites. The proposed algorithm is compared to the ideal situation, where the charging characteristics are perfectly predicted, and to the present benchmark situation where the charging currents are assumed to be equal to the limit set by the EVSE. To ensure the intended operation under realistic conditions, the experiment is carried out using HIL simulations with two commercial EVs and measured data of real charging sessions.

The contributions are as follows:

1. *Illustrating the complexity of the non-ideal charging characteristics.* Unlike other previously mentioned studies regarding the non-idealities, the non-ideal charging characteristics under different current limits set by the EVSE are analysed herein.
2. *Development of an adaptive CCE algorithm* that enables the charging control system to estimate the potentially

unused three-phase charging capacity and reallocate it effectively among the active EVs.

3. *Formulating a simulation model that considers non-ideal charging characteristics.* The simulation model can be used with real EVs (HIL simulation) or without (only simulated EVs).
4. *Comparing the proposed algorithm to the present benchmark solution and to the ideal case.* This can be used to determine the usefulness and optimality of the proposed algorithm.

1.3 | Structure

The controllability of EV charging and the non-ideal charging characteristics are discussed in Section 2. The control algorithm basis and the proposed CCE algorithm are described in Section 3. Section 4 presents the experiment setup, including the HIL simulation model, the used data and the laboratory setup. In Section 5, the results are presented and discussed. Finally, the conclusions are provided in Section 6.

2 | BACKGROUND FOR EV CHARGING CONTROL

The focus herein is on the charging mode 3 defined in the Standard IEC 61851-1. The charging mode 3 includes extended control options while still being cost-efficient, and it is meant to be the basic charging mode for EVs. There may be a need for a charging control also in a fast charging site, but the objective of a fast-charging station is often to provide as much charging power as is safely possible. Consequently, the charging control objective may be different, for example, to utilise an auxiliary battery energy storage system to reduce charging demand peaks from the grid point of view [30]. Therefore, further consideration of fast-charging solutions is not discussed here.

2.1 | Controllability

As stated in [31], mode 3 charging supports currents between 6 and 80 A. To indicate a charging current limit for the EV, the EVSE can adjust the duty cycle of the pulse width modulation signal through the control pilot circuit. The EV should then adjust its charging current to the limit or below it. The same charging current limit is for each phase and thus the EVSE cannot control phases separately.

There are several non-ideal characteristics that can cause a phase current to be lower than the limit indicated by the EVSE. In a three-phase charging point, the most trivial and yet the most impactful issue is the fact that some EVs support only single-phase or two-phase charging. In addition, the OBC or the charging cable may limit the maximum charging current to, for example, 16 A. Other reasons include the OBC reducing the charging current to protect the battery from overheating or the vehicle's battery being nearly fully charge and thus requiring slower charging [14].

2.2 | Nonideal charging characteristics

It may be trivial that different EVs have different charging characteristics. However, an EV may also have different internal charging modes which can affect the charging characteristics of the EV. For example, BMW i3 has three different charging modes: 'maximum', 'reduced' and 'low' [32]. Only the EV user can change the charging mode. Table 1 summarises the examined EVs [33]. Since there are no accurate data available regarding their charging efficiencies, the OBC efficiency is assumed to be the same for each mode of the BMW. Comprehensive details regarding the differences between the three modes of the BMW are not available as it is presumably a trade secret.

The same Smart Grid Technology laboratory [34] and equipment (including the two EVs, the charging point and two energy analysers) are used to measure the realistic non-ideal charging characteristics and to conduct the HIL simulation experiment. The equipment is described in more detail in Section 4.3.

The aim here is not to assess the technical details of the EVs which define their charging characteristics. Instead, the authors illustrate different charging characteristics and discuss their impacts from the charging control system point of view.

2.2.1 | Steady state charging currents

Based on the conducted charging current measurements with different current limits, the charging current seems to be steady (variation of <0.5 A) until around 98% SOC. However, the steady-state currents might be slightly over or notably under the limit set by the charging controller. This is illustrated in Figure 1, where the charging current limit for the BMW in low mode is changed every 20 s. The symbols I1–I3 in the legend represent phase currents. In Figure 1, the largest difference between the limit and the realised charging currents after a 20-s adjustment period is 7.7 A. This is the largest measured deviation between the current limit and the realised charging current of the considered EVs. Similar currents were seen even with longer adjustment periods. This means that the BMW in low mode would charge with currents of around 7.6 A (I1), 7.5 A (I2) and 7.3 A (I3) when the current limit is 15 A. More importantly, Figure 1 shows that all EVs may not be able to use all charging currents between their minimum and maximum supported charging currents, which has been assumed in [16].

For the other BMW modes (i.e. reduced mode and maximum mode), the deviation between the current limit and the realised current is smaller. For the Nissan Leaf, the steady-state single-phase charging currents deviate ± 0.8 A from the current limit. For the sake of conserving space, these are not illustrated.

While the charging characteristics of, for example, BMW's low mode are likely to be more energy efficient or safer from the EV perspective they pose a challenge from the charging control system point of view. This is because there is no standardised way for a charging control system to gain access to the information regarding the charging characteristics of the EVs.

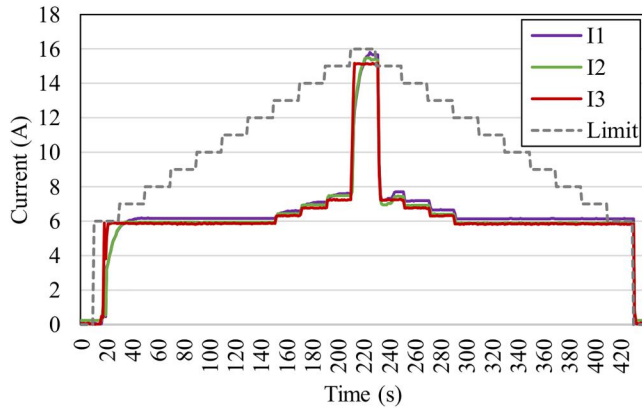
TABLE 1 EV models and charging modes

EV model	Charging mode	Battery capacity	OBC efficiency
BMW i3 (94 AH)	Maximum mode	33.2 kWh	0.865 ^a
	Reduced mode		
	Low mode		
Nissan Leaf	–	24.1 kWh	0.899 ^b

Abbreviations: EV, electric vehicle; OBC, on-board charger.

^aEfficiency for model BMW i3 (120 Ah).

^bEfficiency for model Nissan Leaf Acenta (40 kWh).

**FIGURE 1** Charging characteristics of BMW i3 in low mode

2.2.2 | Adaption time to a new current limit

The steady-state charging current measurements show that it takes around 2–15 s for an EV to reach the new steady state after the current limit changes. The reaction time to decreased current limit seems to be faster, around two seconds for both EVs. A greater change of the current limit does not seem to impact the adaption time. This was seen in the measurements where the current limit is changed in steps of 5 and 10 A. An illustration of these measurements is not included here due to space restrictions.

There seems to be a relatively consistent delay when the charging is supposed to start. This delay is often around 10 s as seen in Figure 1. In three-phase charging, there may also be notable differences between the phases. As shown in Figure 1, one phase current (I3) may react much faster than the others. This characteristic was seen in each measurement of the BMW.

2.2.3 | Charging currents in the final SOCs under a constant current limit

Different EVs may have dissimilar charging characteristics also at the final SOCs. To illustrate this, the final charging curves of both EVs are presented in Figure 2. In this figure, BMW maximum mode is chosen as its final charging curves depend more notably on the current limit compared to the other modes. The illustration of the remaining two modes is excluded to

conserve space. The final charging curves are measured for all current limits (6–16 A), but for the sake of clarity, only the curves with 6, 9, 12 and 16 A limits are presented. In Figure 2b, the three-phase charging of BMW changes into a single-phase charging at around the mid-point of the final charging curve. After the change, the current I1 triples quickly. There seems to be a clear correlation between the steady-state charging current and the point where the three-phase charging changes into a single-phase charging.

The energy drawn during the final charging curve depends notably on the current limit. For the Nissan and the BMW this energy varies between 0.09–0.71 and 0.16–0.91 kWh, respectively. Assuming the efficiencies presented in Table 1, the final charging curves start at around 97.5%–99.7% and 97.5%–99.6% SOC for the Nissan and BMW, respectively.

3 | CHARGING CONTROL ALGORITHM

To overcome the challenges posed by the non-ideal charging characteristics, an adaptive CCE algorithm is proposed. The algorithm utilises real-time charging current measurement as feedback to memorise and deduct the charging characteristics. As opposed to the solution presented in [16], this solution does not require any preliminary data and is computationally light, which are valuable qualities in real-life implementations. The CCE algorithm is designed to complement other charging algorithms to ensure that they operate as intended, even when the EVs have non-ideal charging characteristics. Therefore, an algorithm basis is needed to demonstrate the efficiency of the CCE algorithm. The main objective of the algorithm basis is to:

1. Limit the charging currents according to the limits of the local electricity network
2. Distribute the whole charging capacity evenly between the active EVs.

The algorithm basis is essentially the same as the current benchmark solution used in, for example, [28, 29]. The algorithm does not require any user inputs or preliminary knowledge about the arriving EVs. The following subsection presents the CCE algorithm.

3.1 | Proposed charging characteristic expectation algorithm

In short, the idea of the CCE algorithm is to use charging current measurements to determine the charging characteristics of each active EV, and then use that information to reallocate any potentially unused charging capacity of an EV to other EVs. Modelling each charging session separately makes the algorithm scalable, which is the main issue in the solution presented in [17]. In addition, the modelling considers three-phase charging as opposed to the solution presented in [17] that focuses only on single-phase charging.

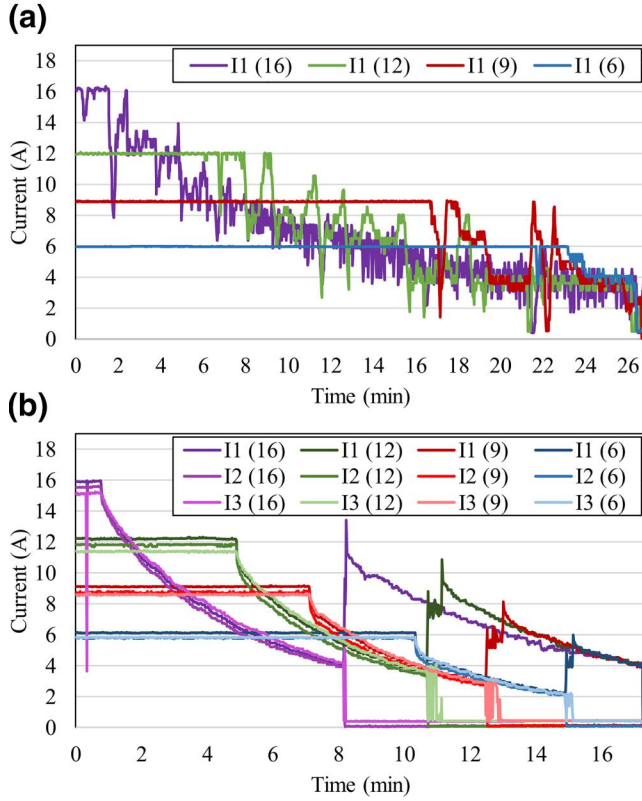


FIGURE 2 Final charging curves for (a) Nissan Leaf and (b) BMW i3 in maximum mode

The charging characteristics model is constituted of a maximum current and a matrix of all current limit-correspondences from 6 A to the maximum current supported by the charging point (e.g. 16 or 32 A). Each current limit-correspondence is constituted of the current limit, phase currents and a Boolean variable. In the beginning of a charging session, when the algorithm notices a change of a charging state from ‘A’ to ‘B’, ‘C’, or ‘D’, the charging characteristics model is initialised, and ideal charging characteristics are assumed. If the charging state is ‘B’, ‘C’ or ‘D’, an EV is connected to the charging point, whereas the state ‘A’ means that an EV is not connected [31]. Further explanation of the standard is not presented here due to space restrictions. The initial charging characteristics model is presented in Figure 3. In the figure, the currents $I_{M,1}$, $I_{M,2}$ and $I_{M,3}$ in the matrix present the presumed currents when the corresponding current limit (I_L) is set by the EVSE. The Boolean variable is used to keep track of which values are actual measurements and which are initial assumptions.

The algorithm begins by updating the charging characteristics model of each active EV based on the current measurements. The updating process is constituted of four different functions: *direct memorisation*, *phase detection*, *maximum current deduction* and *indirect deduction*. These functions are described in the next subsections. After updating the expected charging characteristics, the algorithm calculates

	I_L	$I_{M,1}$	$I_{M,2}$	$I_{M,3}$	Boolean
I_{\max}	6	6.0	6.0	6.0	False
	7	7.0	7.0	7.0	False
	8	8.0	8.0	8.0	False
	\vdots	\vdots	\vdots	\vdots	\vdots
	32	32.0	32.0	32.0	False

FIGURE 3 Initial charging characteristics model

the number of EVs present. This can be done by accessing the charging state information known by the IEC 61851-1 compliant mode 3 charging controller.

After calculating the number of active EVs, the algorithm allocates the available three-phase charging capacity evenly. The capacity distribution process is iterative and considers the charging characteristics memorised and deducted by the CCE algorithm. At the beginning of the distribution process, a 6 A limit is assumed for each active charging session as it is the minimum current limit according to [31]. In each iteration step, the capacity distribution process considers allocating 1 A higher charging current limit for a certain charging session and evaluates whether the expected total charging currents for the charging site will be within the intended limits. If the 1 A higher current limit can be allocated for the charging session, the algorithm updates the considered current limit for the charging session and moves to the next charging session to maintain an even capacity allocation. This will be repeated until a current limit incrementation will result in too high expected total charging currents or until all active charging sessions have the maximum current limits supported by the charging points. This ensures that the non-ideal charging characteristics of each EV are taken into account and the charging capacity will be reallocated if necessary.

Afterwards, there may be single-phase capacity available for allocation and thus the algorithm carries out a similar iterative distribution process for each phase separately. The CCE algorithm deducts the phase usage of each charging session, which makes it possible to optimise phase-specific capacity utilisation. After the algorithm has determined the current limits that are expected to lead to optimal capacity usage rate, the current limits will be sent to the corresponding EVSEs to be put into effect. A simplified block diagram of the control algorithm is presented in Figure 4.

3.1.1 | Direct memorisation

Each time the charging currents are measured, the measurements are updated for the corresponding current limit and the Boolean variable is set to true. An example is given in Figure 5, where the current limit is 10 A and currents of 10.2, 10.1 and 9.9 A are measured afterwards. It should be noted that it may take around 10 s for an EV to properly react to the current limit. Therefore, using a shorter time step may result in an inaccurate charging characteristics model.

The direct memorisation is only memorising the measured values. To improve the rate at which the charging

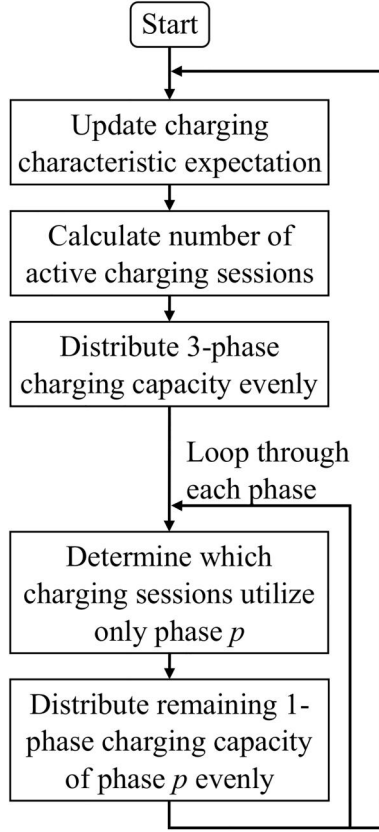


FIGURE 4 Simplified block diagram of the control algorithm

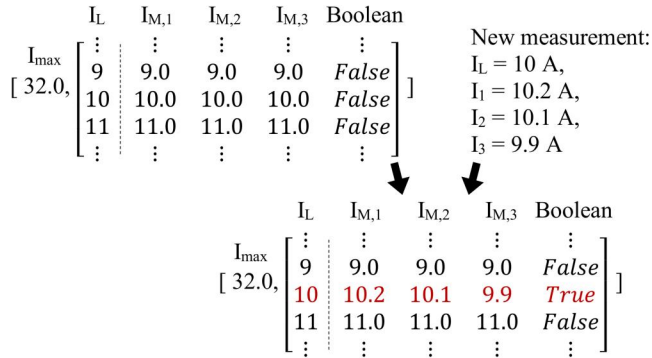


FIGURE 5 Direct memorisation of newly measured charging currents

characteristics modelling evolves, the following three functions use reasonable assumptions made based on the analysis of the non-ideal charging characteristics presented in Section 2.2.

3.1.2 | Phase detection

This function aims to determine which phases are used in the charging session. If one phase current is clearly above zero, while a current on another phase is zero, it means that the phase with zero current is not used. After recognising an unused phase, the charging characteristics model is updated so that there are not assumed to be currents on the phase

regardless of the current limit. An illustration is presented in Figure 6.

There are two key factors which should be considered in this function. First, there may be noise measured by the current metre and thus a small threshold, for example, 1 A, should be used to determine whether a current is zero or not. Second, as mentioned earlier, it may take longer than 10 s for an EV to start charging after the charging is allowed. Therefore, the phase detection function should not be used without a clear delay after the charging is allowed.

3.1.3 | Maximum current deduction

The goal of this function is to determine the highest current that an EV can use. Public charging points may very well be suitable for charging currents of up to $3 \times 32 \text{ A}$, but EVs with $\leq 16 \text{ A}$ maximum supported charging current in mode 3 (IEC 61851-1) are very common. Since it is very likely that most EVs cannot utilise the higher end currents, the accuracy of the charging characteristics model may be improved notably after deducting the maximum charging current.

The maximum current deduction function checks if the measured charging current is clearly below the set current limit. And, if so, the measured current is assumed to be the maximum charging current for the present EV. As shown in Figure 1, there may be notable differences ($>7 \text{ A}$) between the current limit and the charging current even though the current has not reached its maximum value. Therefore, a threshold of a couple of amperes should be used to determine whether there is a clear difference between the current limit and the measured charging current. However, since the algorithm can always relearn the maximum charging current for each session, there is no need for a remarkably high threshold (e.g. $>7 \text{ A}$) which would minimise the risk of erroneous maximum charging current deduction.

The maximum current is taken into account according to Equation (1), where I_E represents the expected charging current, I_M represents the corresponding currents in the matrix, I_{\max} represents the maximum current, L denotes the considered current limit, and the subscript p denotes the phase.

$$I_{E,p}(L) = \min[I_{M,p}(L), I_{\max}]. \quad (1)$$

3.1.4 | Indirect deduction

The aim of this function is to improve the modelling accuracy of those current limit-correspondences which are yet not directly measured but which are between two directly measured current limit-correspondences. Since the non-measured current limit-correspondences are assumed to be ideal, they may be significantly inaccurate (potentially over 7 A difference as shown in Figure 1). The current limit-correspondences seems

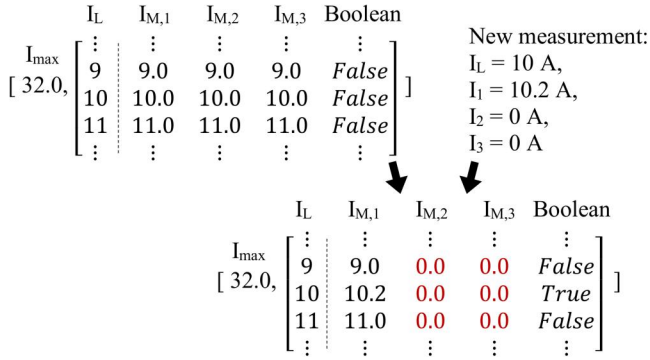


FIGURE 6 Detection of unused phases in the present charging session

to be logical in a way that a higher current limit results in equal or higher charging currents, whereas a lower current limit results in equal or lower charging currents. Therefore, two directly measured current limit-correspondences can be used to determine boundaries for all non-measured correspondences between them. Since more accurate prediction becomes very complex and requires more input data, it is reasonable to assume that the non-measured current limit-correspondences are settled linearly between the two directly measured correspondences.

After receiving a current measurement, the indirect deduction function is used to check whether there are non-measured current limit-correspondences between the adjacent directly measured correspondences. This is made possible with the Boolean variables. If a measured correspondence is found after one or more non-measured correspondences, the non-measured correspondences are updated. The operation of this function is illustrated in Figure 7.

4 | EXPERIMENT

In order to ensure compliance with commercial EVs, the verification of the charging control algorithm is carried out using HIL simulations. To further improve the overall accuracy of the simulation model, real charging behaviour data and realistic charging characteristics (illustrated in Section 2.2) are used. The following subsections describe the used simulation model, modelling of charging characteristics, the laboratory setup and the simulation case.

4.1 | Simulation model

The experiment consists of up to two HIL charging points, which are described in Section 4.3, and a necessary amount of fully simulated charging points. The key feature of the simulation model is the coupling of realistic charging profiles (Section 4.2) and real charging session data (Section 4.4). The simulation model and the used algorithms are implemented using Python programming language, and a time step of 10 s is

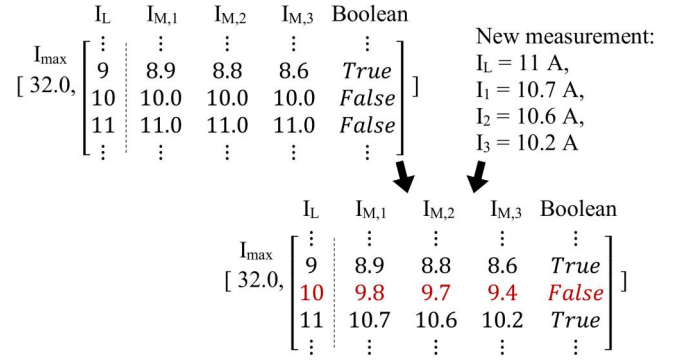


FIGURE 7 Indirect charging characteristics deduction

used to calculate the values of the simulated EVs and to measure the charging currents of the HIL charging points.

The control algorithm is run every 60 s unless a new EV arrival is observed. To avoid potential overloading, the control algorithm does not allow charging for a new charging session until the control algorithm has allocated the charging capacity properly. In the case of a new EV arrival, the control algorithm is run on the very next time step. This improves the EV user convenience as the charging will start with minimal delay.

As mentioned in Section 2.2, there may be a delay of over 10 s before a charging session starts properly. Therefore, the algorithm waits 1 min after the start of the charging sessions before enabling *phase detection* and *maximum current deduction* functions to avoid erroneous characteristics deduction.

4.2 | Modelling of EV charging profiles

This subsection describes the modelling of the charging profiles in the simulation model and should not be confused with charging characteristics modelled by the CCE algorithm. The charging profiles are modelled based on the measurements illustrated in Section 2.2. Another option to model battery behaviour would be the use of equivalent circuit models (ECM). However, this approach is problematic as the detailed parameters of an ECM as well as the battery pack composition are generally trade secrets of the manufacturers and cumbersome to determine via experimental battery measurements and reverse engineering [16]. The charging profiles are measured for each current limit for both EVs and for each BMW charging mode mentioned in Table 1. The currents, voltages and time are then used to calculate the missing energy of the EV battery. The energies, currents and current limits are then used to determine realistic charging profiles for each EV (and for each BMW's charging mode) in which the charging current depends on the EV battery energy level and the charging current limit set by the charging controller.

The impacts of the battery temperature and other external factors are not considered in these models. Therefore, a slight deviance between the modelled charging currents and the

laboratory measurements is expected. However, the charging profiles can still be used to introduce realistic non-ideal charging characteristics to the simulation model.

4.3 | Laboratory setup

The experiment was carried out at the Smart Grid Technology Lab [34] at TU Dortmund University. The HIL simulations used the same EVs described in Table 1. A modified RWE eSTATION charging station with two charging sockets suitable for up to 22 kW (400 V AC) charging power was used. The charging station included two Phoenix Contract Advanced EV Charge Controllers (type EM-CP-PP-ETH) which are compatible with IEC 61851-1 standard.

The algorithm uses a Modbus library (PyModbus [35]) which enables it to control the charging current limits of the charging controllers and to read registers such as the charging state. A similar Modbus connection is used for two KoCoS EPPE PX power quality analysers with KoCoS ACP 300 current probes to measure phase voltages and charging currents. The setup for the HIL simulations is illustrated in Figure 8, and a photograph of the setup is presented in Figure 9.

While the run time of one loop of the script (including the proposed CCE algorithm) is a fraction of a second, the queries through the Modbus connection may occasionally take several seconds. The selected time step of 10 s works well without any issues but the tests with shorter time steps does show an increasing chance of the queries not having enough time to receive a response.

4.4 | Simulation case

The simulation case uses real charging data measured at Mall of Tripla [36], which is located in Helsinki, Finland. There are nearly 300 charging points, and the charging points for public use can supply charging powers up to 22 kW. The data consist of around 5000 charging sessions recorded over a 6-month period (October 2019–March 2020). The charging sessions were uncontrolled. The data include start time, stop time, energy consumption and peak power of each charging session.

According to the charging data, there were up to 20 simultaneous charging sessions. Since the utilisation rate of the charging infrastructure was so low, the simulations consider only 20 charging points and a total charging capacity limit of 3×120 A. As a consequence, the algorithm basis mentioned in Section 3 is needed to limit the charging currents during congestions. Since there are always at least 3×6 A charging capacity for each charging session, there is no need to temporarily disable any charging sessions.

The simulations consider three scenarios. These scenarios are based on the 3 days with the highest number of charging sessions and the highest total energy consumptions. By assuming that the peak power of three-phase charging would be over 10 kW, the EV types (single-phase or three-phase) can be estimated. Scenarios 1 and 2 represent the days with the highest

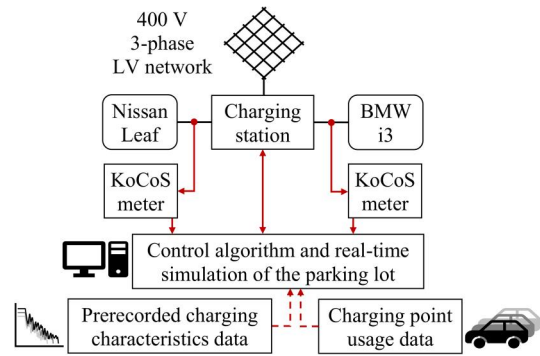


FIGURE 8 The setup for the hardware-in-the-loop (HIL) simulations. HIL, hardware-in-the-loop



FIGURE 9 The laboratory setup

number of single-phase and three-phase charging sessions, respectively, whereas Scenario 3 represents the day with the highest energy consumption. All single-phase charging sessions are modelled based on the Nissan, whereas all three-phase charging sessions are modelled based on the BMW. The BMW modes for the three-phase charging sessions are chosen arbitrarily. The scenarios are presented in Table 2, and the charging point occupation rate is illustrated in Figure 10. Since these charging sessions are uncontrolled, their total charged energies are used as a reference value to represent the 100% QoCS level used herein for comparison purposes. For each examined algorithm, the QoCS is calculated by dividing its total charged energy with the total charged energy of the uncontrolled case.

In addition to these scenarios, simulations are conducted to provide an example of a peak power-based charging control algorithm and to demonstrate its differences regarding the capacity allocation. This example is based on Scenario 3, but the charging capacity is limited to 82.8 kW, which equals an average phase current of 120 A (230 V). However, in this case, the fuse size is assumed to be higher, and thus, the currents on the individual phases are allowed to rise above 120 A as long as the total charging load is within the power limit. In the future, peak power-based electricity tariffs are likely to become more popular as they improve the cost-reflectivity of the electricity pricing [37]. As a result, there will be an incentive to limit peak loading in charging sites and thus effective capacity utilisation becomes more valuable.

TABLE 2 Scenarios

	Number of electric vehicle charging sessions	Three-phase charging sessions	Single-phase charging sessions	Total charged energy	Date
1.	66	4	62	372 kWh	22 Feb 2020
2.	61	12	49	428 kWh	19 Oct 2019
3.	59	10	49	454 kWh	14 Dec 2019

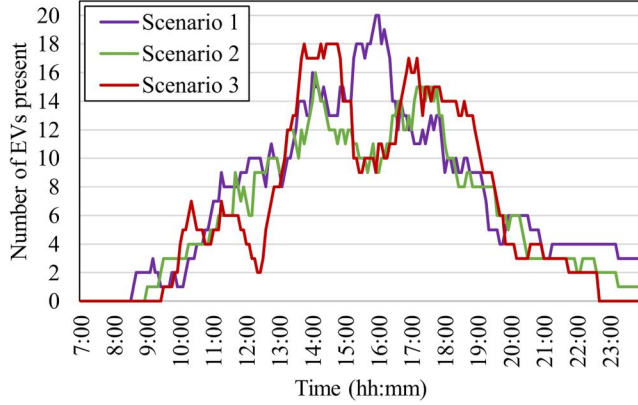


FIGURE 10 Charging point utilisation for Scenarios 1–3

5 | RESULTS

The simulations are carried out using four different algorithms:

Algorithm 1 *Uncontrolled charging*

Algorithm 2 *Control without an adaptive CCE algorithm (the present benchmark solution),*

Algorithm 3 *Control with the proposed CCE algorithm*

Algorithm 4 *Control with perfect knowledge of the charging characteristics*

The same algorithm basis (presented in Section 3) is used for Algorithms 2–4, and only the adaption method to the different charging characteristics varies. The second algorithm does not include an adaptive CCE algorithm and thus the control algorithm essentially assumes charging characteristics of each EV to stay ideal. The third algorithm utilises the proposed CCE algorithm. The fourth algorithm has perfect knowledge about the charging characteristics and battery energy levels. Due to the required preliminary knowledge, the fourth algorithm can only be simulated. As the first two algorithms are less complex, only the third algorithm is carried out as an HIL simulation. However, the charging requirements of the EVs are kept the same regardless of the chosen algorithm. The fourth algorithm is used to assess the optimality of the proposed CCE algorithm and to determine the upper bound of the possible capacity usage rate without the risks of overloads. The capacity usage rate (C_{usage}) is calculated according to Equation (2), where t is time index, P is

the realised power consumption and P_{max} is the maximum allowed power determined based on, for example, the fuse size or other peak load limit.

$$C_{\text{usage}}(t) = \frac{P(t)}{P_{\text{max}}(t)}. \quad (2)$$

5.1 | Scenarios 1–3

The results of Scenarios 1–3 are summarised in Table 3. The charging loads in Scenario 1 and 2 are naturally spread over the day, and thus, even the uncontrolled charging load peak is relatively modest. However, Algorithm 2 simply divides the available charging capacity among the EVs without recognising that some of the EVs draw much lower currents than the limit set by the EVSEs. Since the unused capacity is not reallocated to other EVs, it is essentially wasted, resulting in lower QoCS.

In Scenario 3, there is a notable charging load congestion between 13:30 and 14:48 h and a smaller congestion between 16:42 and 17:13 h. In the case of uncontrolled charging, the highest current peaks at 144 A, which means an overload of 24 A (20%), and thus, a peak load limitation is necessary. The currents in case of Algorithms 3 and 4 are very similar and thus the proposed CCE feature seems to operate near ideally. According to the simulations, even Algorithm 4 results in a slight QoCS reduction of 8.1 kWh (1.8%), whereas Algorithms 2 and 3 resulted in a QoCS reduction of 148.2 (32.6%) kWh and 9.7 (2.1%) kWh, respectively. The currents in Scenario 3 are presented in Figure 11.

To illustrate the charging currents in more detail, the moment of the more notable congestion is presented in Figure 12. Algorithms 3 and 4 result in very similar charging currents. Since the control algorithms are run only every 60 s or in the case of a new EV arrival, neither algorithms can fully utilise the whole charging capacity without the risk of a slight overload. In addition, the charging sessions are not likely to be equally distributed for the three phases, which may lower the optimal capacity usage rate. The average capacity usage rates during 13:30–14:40 h are 45.4%, 87.9% and 88.9% for the Algorithms 2–4, respectively.

5.2 | Peak power-based capacity allocation

This example demonstrates that a peak power limit-based charging capacity allocation is more straightforward than, for example, fuse size-based capacity allocation. This is because a

TABLE 3 Results of Scenarios 1–3

Scenario	Algorithm	QoCS	Charged energy	Uncharged energy
1.	1.	100.0%	372.1 kWh	0.0 kWh
	2.	77.6%	288.8 kWh	83.3 kWh
	3.	100.0%	371.9 kWh	0.2 kWh
	4.	100.0%	372.0 kWh	0.1 kWh
2.	1.	100.0%	427.8 kWh	0.0 kWh
	2.	84.5%	361.4 kWh	66.4 kWh
	3.	100.0%	427.8 kWh	0.0 kWh
	4.	100.0%	427.8 kWh	0.0 kWh
3.	1.	100.0%	454.3 kWh	0.0 kWh
	2.	67.4%	306.0 kWh	148.2 kWh
	3.	97.9%	444.6 kWh	9.7 kWh
	4.	98.2%	446.1 kWh	8.1 kWh

Abbreviation: QoCS, quality of the charging service.

power-based capacity allocation does not require perfectly balanced load for each phase. Therefore, a higher capacity usage can be achieved. However, it is still necessary to consider each phase separately to avoid phase-specific overloading, and an adaptive CCE algorithm is still required to effectively allocate the intended total charging capacity. In this case, 96.5% average capacity usage is achieved during 13:30–14:40 with the proposed CCE algorithm. The charging currents are presented in Figure 13. Without an adaptive CCE algorithm, the capacity usage would be 45.4%, whereas the ideal algorithm would result in 98.0% capacity usage rate over the same period. The QoCS for Algorithms 2–4 are 67.4%, 99.8% and 99.9%, respectively.

It is worth mentioning that even a higher capacity usage percent is possible by exploiting the fact that in some cases, such as [17], the objective is to limit the average power of a 1-h long period to a certain level, and thus, the power is allowed to momentarily be higher than the targeted level.

5.3 | Discussion

Based on the results, by not considering an adaptive CCE algorithm over half of the charging capacity would remain unused. In addition, even an ideal algorithm may not achieve higher a fuse size-based maximum capacity usage rate than 89%. This is because of the unevenly balanced charging loads and the non-ideal EV charging characteristics, which reduces the controllability of the charging load. When comparing Algorithm 3 (the proposed CCE algorithm) and Algorithm 2 (the present benchmark solution), the average charged energy is increased by 96.0 kWh by the CCE algorithm. Consequently, the average QoCS is improved from 76.5% to 99.3%. These results underline the usefulness of the CCE algorithm to maximise the QoCS while minimising the investment costs of the required charging infrastructure. When comparing the

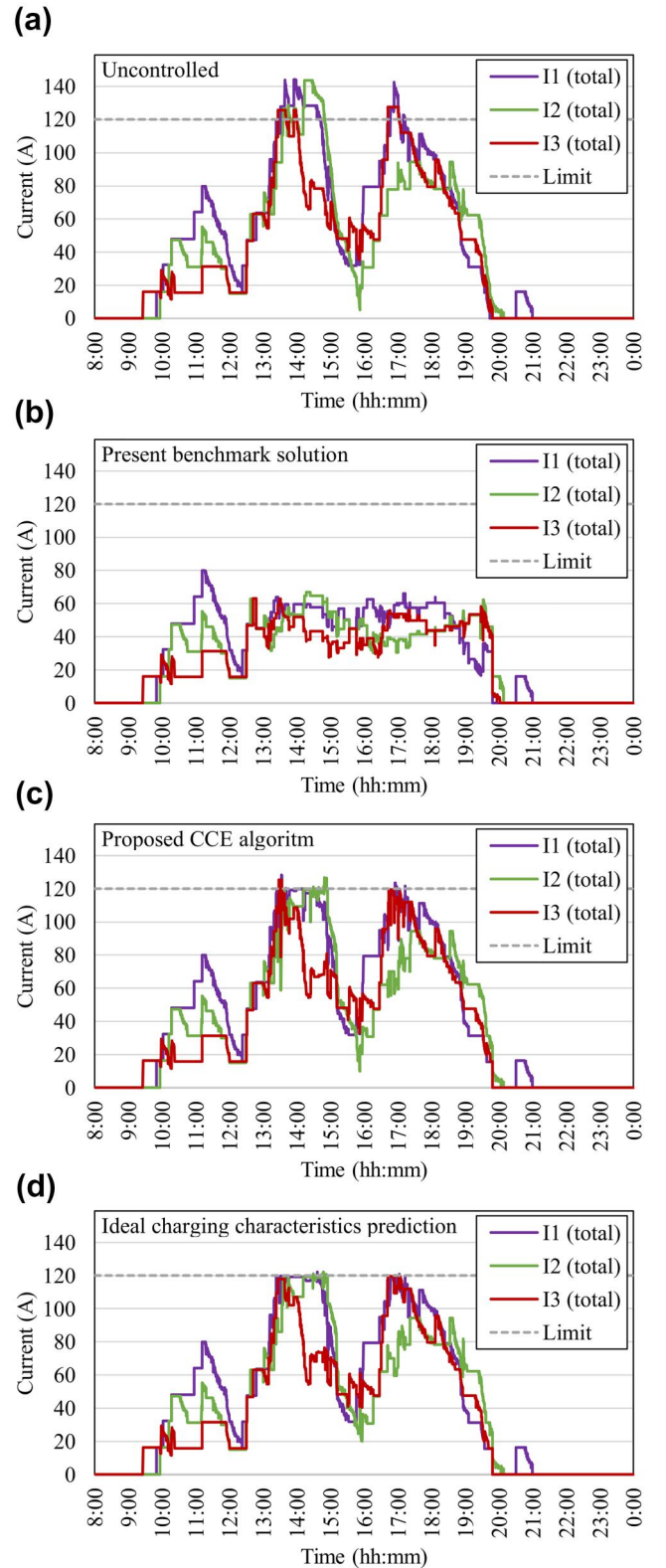


FIGURE 11 Charging currents in Scenario 3 in the case of (a) Algorithm 1, (b) Algorithm 2, (c) Algorithm 3 and (d) Algorithm 4

CCE algorithm to Algorithm 4 (perfect preliminary knowledge of the charging characteristics), the average charged energy is only 0.6 kWh higher with Algorithm 4. The average QoCS is

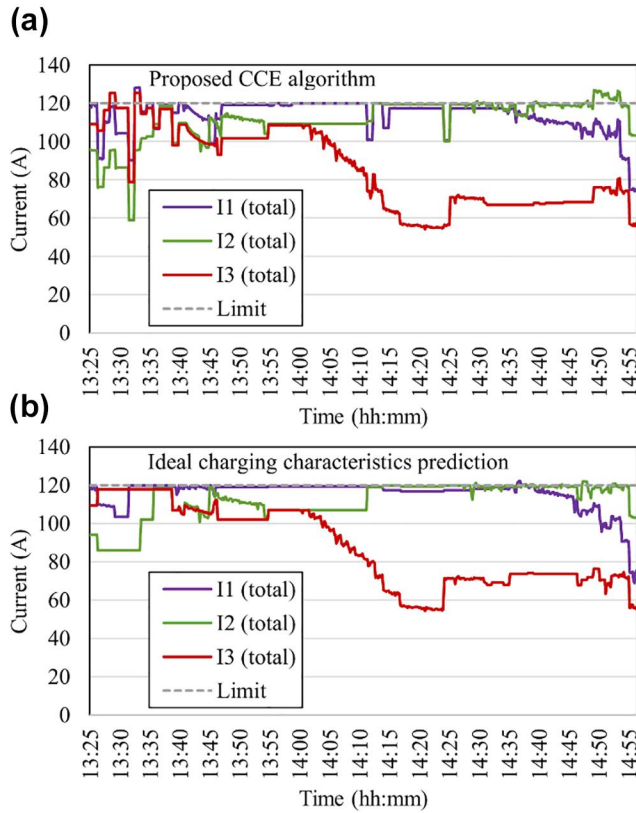


FIGURE 12 Charging currents in Scenario 3 between 13:25 and 14:55 in case of (a) Algorithm 3 and (b) Algorithm 4

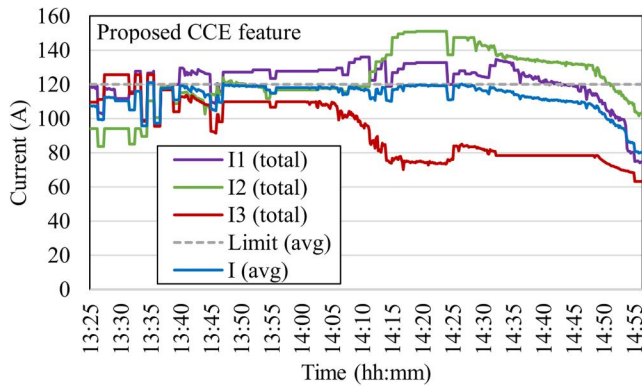


FIGURE 13 Charging currents in a power capacity allocation example utilising the proposed charging characteristics expectation (CCE) algorithm in Scenario 3. CCE, charging characteristics expectation

99.4% with Algorithm 4. Based on these results, it can be seen that the proposed CCE algorithm overcomes the issues posed by the non-ideal charging characteristics near ideally.

The non-ideal charging characteristics would particularly affect the algorithms that schedule the charging of EVs based on their individual energy requirements and departure times, such as the algorithms presented in [1, 2, 4, 11, 24]. The impacts to the individual EVs cannot be completely avoided but the proposed CCE algorithm could be used to ensure that the

whole intended charging capacity is used efficiently, which will improve the average QoCS of all EVs.

It is worth mentioning that the charging standard IEC 61851 supports digital data communication between the EV and the EVSE which, in theory, could replace the need for the proposed CCE algorithm. However, this communication approach is problematic from two perspectives. First, the charging characteristics are complex, and the charging current depends on variables such as the temperature. In addition, the correlation between the charging current and the current limit set by the EVSE is not always linear as presented in Figure 1. Thus, in order to accurately keep track of the charging characteristics of an EV, the control system requires multiple updated data sets of the charging characteristics throughout every charging session. This would increase the data transfer between EV, EVSE, and the control system notably. Second, even if the data transfer would be supported by some of the EVs in the near future, it might take a long time for all EVs to be able to support this data transfer. In the meantime, the proposed solution will be very valuable. Based on the optimality of the proposed solution, it may even be argued that there is no need for EVs to be able to inform the EVSE or the main control system about their charging characteristics.

The vehicle-to-X (V2X) is not considered herein as it is not supported by the used EVs and charging point. It is reasonable to assume that the V2X operation also includes non-ideal characteristics that will limit its controllability. The proposed CCE algorithm could be modified relatively easily to consider V2X operation. However, to ensure its effective operations, it should be tested using EVs and charging points that support bidirectional power flow.

6 | CONCLUSIONS AND FUTURE WORK

The often-overlooked issues caused by the non-ideal charging characteristics of commercial EVs have been illustrated and discussed herein. While the non-ideal charging characteristics may make the charging safer and more energy efficient from the EV's perspective, they pose a challenge from the charging control system point of view. There is currently no standardised way for a control system to gain access to the information regarding the EVs' charging characteristics. Therefore, an adaptive CCE algorithm seems to be a prominent solution to ensure that the intended charging capacity is effectively used in public charging sites.

An adaptive CCE algorithm is proposed herein. The algorithm utilised charging current measurements to memorise and deduct charging characteristics of the EVs without any preliminary knowledge. This information is then used to ensure that the intended capacity is effectively used resulting in a higher quality of charging service. The proposed CCE algorithm is tested using HIL simulations with commercial EVs to ensure compliance with the standard IEC 61851-1. In order to test the operation in a larger charging site, a simulation model is developed that couples realistic charging profiles

(charging current over time) with real charging data (arrival time, departure time and energy requirement). Thus, the simulation model ensures that the non-ideal charging characteristics, which cause the charging current to deviate from the current limit set by the EVSE, are realistically modelled.

According to the simulation results, the proposed CCE algorithm operates almost as well as the ideal algorithm with perfect knowledge. When compared to the present benchmark solution, the total daily charging energy is increased by 96 kWh on average, resulting in the average QoCS increasing from 76% to 99%. In addition, the results show that the proposed CCE algorithm reaches up to 88% maximum charging capacity usage rate over the congestion hour if the capacity is determined by a fuse size, whereas the ideal control algorithm reaches 89% and the present benchmark solution reaches only 45%. If the available charging capacity is limited to a certain peak power, the capacity allocation does not require perfectly balanced phase loading. Therefore, the capacity allocation is simpler and a higher capacity usage rate is possible. In this case, the proposed CCE algorithm reaches the 97% maximum capacity usage rate.

The result also gives an indication that over 98% QoCS can be achieved in a public charging site with multiple 22 kW charging points even if the total charging capacity per charging point results in 3×6 A. To determine more comprehensive guidelines to maximise the QoCS while minimising the investment costs of the necessary charging infrastructure at public charging sites, extended simulations will be carried out for different charging sites. Additional future works include testing of the proposed CCE algorithm in a pilot case with multiple charging points and analysis of non-ideal discharging characteristics in V2X operation.

ACKNOWLEDGEMENTS

This work was supported by the LIFE Programme of the European Union (LIFE17 IPC/FI/000002 LIFE-IP CANEMURE-FINLAND). The work reflects only the authors' views and the EASME/Commission is not responsible for any use that may be made of the information it contains. Kalle Rauma would like to thank the support of the German Federal Ministry of Transport and Digital Infrastructure through the project 'PuLS—Parken und Laden in der Stadt' (03EMF0203B). The authors would like to thank IGL Technologies for providing charging data and contributing ideas for the work.

CONFLICT OF INTEREST

The authors declare that they have no known competing financial interests or personal relationships that could have appeared to influence the work reported herein.

ORCID

Toni Simolin  <https://orcid.org/0000-0002-0254-1113>

REFERENCES

1. Yang, Y., et al.: Decentralised EV-based charging optimization with building integrated wind energy. *IEEE Trans. Automat. Sci. Eng.* 16(3), 1002–1017 (2019)
2. Koufakis, A.M., et al.: Offline and online electric vehicle charging scheduling with V2V energy transfer. *IEEE Trans. Intell. Transport. Syst.* 21(5), 2128–2138 (2020)
3. Bryden, T.S., et al.: Electric vehicle fast charging station usage and power requirements. *Energy*. 152, 322–332 (2018)
4. Wei, Z., et al.: Intelligent parking garage EV charging scheduling considering battery charging characteristic. *IEEE Trans. Ind. Electron.* 65(3), 2806–2816 (2018)
5. Su, J., Lie, T.T., Zamora, R.: Modelling of large-scale electric vehicles charging demand: a New Zealand case study. *Electr. Power Syst. Res.* 167, 171–182 (2019)
6. Calearo, L., et al.: Grid loading due to EV charging profiles based on pseudo-real driving pattern and user behavior. *IEEE Trans. Transp. Electrific.* 5(3), 683–694 (2019)
7. Liu, Y., Deng, R., Liang, H.: A stochastic game approach for PEV charging station operation in smart grid. *IEEE Trans. Ind. Inf.* 14(3), 969–979 (2018)
8. Bulut, E., Kisacikoglu, M.C., Akkaya, K.: Spatio-temporal non-intrusive direct V2V charge sharing coordination. *IEEE Trans. Veh. Technol.* 68(10), 9385–9398 (2019)
9. Kim, J.D.: Insights into residential EV charging behavior using energy metre data. *Energy Pol.* 129, 610–618 (2019)
10. Fotouhi, Z., et al.: A general model for EV drivers charging behavior. *IEEE Trans. Veh. Technol.* 68(8), 7368–7382 (2019)
11. Zhang, G., Tan, S.T., Wang, G.G.: Real-time smart charging of electric vehicles for demand charge reduction at non-residential sites. *IEEE Trans. Smart Grid.* 9(5), 4027–4037 (2018)
12. Quiros-Tortos, J., et al.: Statistical representation of EV charging: real data analysis and applications. 20th Power Systems Computation Conference (PSCC), pp. 1–7. Dublin, Ireland, June (2018)
13. Zeng, T., Zhang, H., Moura, S.: Solving overstay and stochasticity in PEV charging station planning with real data. *IEEE Trans. Ind. Inf.* 16(5), 3504–3514 (2020)
14. Lee, Z.J., et al.: Large-scale adaptive electric vehicle charging. *IEEE Global Conference on Signal and Information Processing (GlobalSIP)*, Anaheim, CA, USA, 863–864 (2018)
15. Sun, C., et al.: Classification of electric vehicle charging time series with selective clustering. *Electr. Power Syst. Res.* 189, 106695 (2020)
16. Frendo, O., et al.: Data-driven smart charging for heterogeneous electric vehicle fleets. *Energy AI.* 1, 100007 (2020)
17. Simolin, T., et al.: Optimised controlled charging of electric vehicles under peak power-based electricity pricing. *IET Smart Grid.* 3(6), 751–759 (2020)
18. Ucer, E., et al.: An Internet-inspired proportional fair EV charging control method. *IEEE Syst. J.* 13(4), 4292–4302 (2019)
19. Xydas, E., Marmaras, C., Cipcigan, L.M.: A multi-agent based scheduling algorithm for adaptive electric vehicles charging. *Appl. Energy.* 177, 354–365 (2016)
20. Lam, A.Y.S., Leung, K.C., Li, V.O.K.: Capacity estimation for vehicle-to-grid frequency regulation services with smart charging mechanism. *IEEE Trans. Smart Grid.* 7(1), 156–166 (2016)
21. Wan, Z., et al.: Model-free real-time EV charging scheduling based on deep reinforcement learning. *IEEE Trans. Smart Grid.* 10(5), 5246–5257 (2019)
22. Ma, W.J., Gupta, V., Topcu, U.: Distributed charging control of electric vehicles using online learning. *IEEE Trans. Automat. Control.* 62(10), 5289–5295 (2017)
23. Lopez, K.L., Gagne, C., Gardner, M.A.: Demand-side management using deep learning for smart charging of electric vehicles. *IEEE Trans. Smart Grid.* 10(3), 2683–2691 (2019)
24. Sadeghianpourhamami, N., Deleu, J., Develder, C.: Definition and evaluation of model-free coordination of electrical vehicle charging with reinforcement learning. *IEEE Trans. Smart Grid.* 11(1), 203–214 (2020)
25. Zhang, X., et al.: Deep-learning-based probabilistic forecasting of electric vehicle charging load with a novel queuing model. *IEEE Trans. Cybern.* 1–14 (2020)

26. Li, H., Wan, Z., He, H.: Constrained EV charging scheduling based on safe deep reinforcement learning. *IEEE Trans. Smart Grid.* 11(3), 2427–2439 (2020)
27. Silva, F.L.D., et al.: Coordination of electric vehicle charging through multiagent reinforcement learning. *IEEE Trans. Smart Grid.* 11(3), 2347–2356 (2020)
28. Heredia, W.B., et al.: Evaluation of smart charging for electric vehicle-to-building integration: a case study. *Appl. Energy.* 266, 114803 (2020)
29. Zhang, T., et al.: Real-time renewable energy incentive system for electric vehicles using prioritisation and cryptocurrency. *Appl. Energy.* 226, 582–594 (2018)
30. Gjelaj, M., et al.: Optimal infrastructure planning for EV fast-charging stations based on prediction of user behaviour. *IET Electr. Syst. Transp.* 10(1), 1–12 (2020)
31. International Standard IEC 61851-1: Electric vehicle conductive charging system—Part 1: General requirements (2017)
32. BMW AG: The BMW i3. Owners Manual, pp. 183. Munich, Germany (2015)
33. Electric vehicles in test: this is how high the power consumption is. (In germany: Elektroautos im Test: So hoch ist der Stromverbrauch). <https://www.adac.de/rund-ums-fahrzeug/tests/elektromobilitaet/stromverbrauch-elektroautos-adac-test/>. Accessed 13 April 2021
34. Spina, A., et al.: Smart grid technology Lab - a full-scale low voltage research facility at TU Dortmund university. 2018 AETT International Annual Conference, Bari, Italy. pp. 1–6 (2018)
35. PyModbus—A Python Modbus Stack. <https://pymodbus.readthedocs.io/en/latest/readme.html#>. Accessed 13 April 2021
36. Parking at Tripla. <https://malloftripla.fi/en/pysakointi>. Accessed 13 April 2021
37. Lummi, K., Mutanen, A., Järventausta, P.: Upcoming changes in distribution network tariffs—potential harmonisation needs for demand charges. 25th International Conference on Electricity Distribution (CIRED), Madrid, Spain, pp. 3–6. (2019)

How to cite this article: Simolin T, Rauma K, Rautiainen A, Järventausta P, Rehtanz C. Foundation for adaptive charging solutions: Optimised use of electric vehicle charging capacity. *IET Smart Grid.* 2021;1–13. <https://doi.org/10.1049/stg2.12043>